Analytic Determination of the Roller Length of a Hydraulic Jump in an Open Channel Flow using a Bouncing Ball

Abstract

A hydraulic jump is a natural occurrence that occurs in spillways, rivers, and other open channel flows when water or other liquid flowing with a high velocity discharges into a region of lower velocity with an attendant abrupt rise in the liquid surface. Such a phenomenon is normally accompanied by substantial dissipation of energy wherever it occurs. Hydraulic jump is a current method of choice for the safe discharge of floodwater due to its inherent ability to safely dissipate substantial energy. Investigators, in the past, focused their attention on the study of the hydraulic jump, under varied working situations, that resulted to rise in energy loss in open channel structures. In this paper, the author developed numerical two models to calculate the lengths of hydraulic jumps in a horizontal open channel flow using a bouncing ball. The models were based on the laws of motion and the principles of impulse and momentum, to predict the length of a hydraulic jump in a horizontal open channel flow with the Froude number between 2.25 and 15.96. The models were then verified with the experimental data obtained in a large-size facilities. Results showed that the values of the hydraulic jump were reasonable predicted from the models with the Pearson correlation coefficients of between 0.992 and 0.997.

Keywords: Open channel flow, Bouncing ball, hydraulic jump length, law of motion, Froude Number

1 Introduction

A hydraulic jump is a natural occurrence that occurs when there is a flow impediment, such as a weir, bridge abutment, sluice gates, spillways, rivers, and other open channel flows, downstream to water or other liquid flowing with a high-velocity supercritical flow discharges into a region of lower velocity subcritical flow with an attendant abrupt rise in the liquid surface.

The phenomenon is normally accompanied by substantial dissipation of energy wherever it occurs and is hence, the design engineers preferred option for energy dissipation below spillways and outlets. An appropriately planned hydraulic jump can deliver up to 60-70% energy dissipation in the stilling basin alone, thereby restraining the destruction of structures and the streambed.

Several studies, including Rouse et al (1959), Resch and Leutheusser (1972a,1972b), Chanson and Brattberg (2000), Liu al (2004), Lennon and Hill (2006), Chanson (2007), and Kucukalli and Chanson (2008), measured the turbulence in hydraulic jumps.

An enormous amount of air is trapped during a hydraulic jump (Rajaratnam, 1962, 1967; Wisner, 1965). The air is trapped at the jump toe, which signifies a separation between the impinging flow and the roller.

In a hydraulic jump roller, the air-water shear area and the upper free-surface layer can be distinguished as two discrete air entrainments at high Froude numbers.

Rajaratnam (1962) carried out the first effective air-water flow measurements in hydraulic jumps.

The strength of the jump, which is usually determined by Froude Number, is classified as:

1.1. Undular hydraulic Jump when the Froude number of the flow is between 1 and 3. This type of hydraulic jump is weak and no noteworthy water level rise is detected.

1.2. Weak hydraulic jump when the Froude number is between 3 and 6. A weak jump takes place when the velocity in water is very low and the water particles cannot be stable and flow in various ways.

1.3. Oscillating Hydraulic Jump occurs when the Froude Number is 6 and 20. An oscillating jump forms when an oscillating jet enters into a supercritical state and there the number of particles starts oscillating in a clockwise or either anticlockwise direction, forming slighter tides or waves to the top surface. In addition, the flow is dependent on a heavy blow of air in one direction.

1.4. Steady Hydraulic Jump occurs when the Froude Number is between 20 and 80. In a steady jump, the bed surface is quite rough so the particles start to tend in one direction with heavy velocity and turbulence; frictional losses are more in this type of jump.

1.5. Strong Hydraulic Jump when the Froude Number is greater than 80. A strong jump is a perfect jump formed when frictional losses are more, air pressure division is equal and velocity is very high that losses take place. The water changes its state from supercritical to subcritical in a much shorter length when compared to all other types of hydraulic jumps, so this jump is highly preferred in dam structures. A strong jump is a perfect jump formed when frictional losses are more, air pressure division is equal and velocity is very high that losses take place. The water changes its state from supercritical to subcritical in a much shorter length when compared to all other types of hydraulic jumps, so this jump is highly preferred in dam structures.

Applying the equations of conservation of mass and momentum in integral form to a hydraulic leap in a straight horizontal rectangular channel yields two relationships between the conjugate flow properties or the properties upstream and downstream of the jump [6, 8].

$$\frac{d_2}{d_1} = \frac{1}{2}\left[\sqrt{1 + 8Fr_1^2} - 1\right] \qquad \frac{Fr_2}{Fr_1} = \frac{2^{3/2}}{\left(\sqrt{1 + 8Fr_1^2} - 1\right)^{3/2}}$$

where the Froude number is Fr and d is the water depth, g is the gravity constant, V is the flow velocity, and the subscripts 1 and 2 are the upstream and downstream flow parameters, respectively, in the formula: Fr = V/(gd)1/2. With a few notable examples, the major part of earlier hydraulic jump investigations was carried out with rather large inflow Froude numbers ($Fr_1 > 3$), due to their design implications.

The Reynolds number is defined as $Re = 4V_1R/v$ with V_1 as the velocity and R as the hydraulic radius at the toe of the jump and the dynamic viscosity of water.

In the equation: d is the water depth, g denotes the gravitational constant, V denotes the flow velocity, and subscripts 1 and 2 denote the upstream and downstream flow parameters, respectively.

Several researchers like Rouse et al (1959), Resch and Leutheusser (1972a, 1972b), Chanson and Brattberg (2000), Liu et al. (2004), Lennon and Hill (2006), Chanson (2007) and Kucukali and Chanson (2008) conducted turbulence measurements in hydraulic jumps.

Their studies concentrated either on the turbulent water flow properties with relatively low Froude number situations or on the air-water flow properties in the jump roller.

Other researchers like Safranez (1929), and Baje (1965) developed models that predicted roller lengths of hydraulic jumps.

Numerical modeling of hydraulic jumps was the subject of a few researches, while the air-water flow parameters were examined under a few specific circumstances. The size and temporal scales of turbulent structures are essential details to explain turbulent processes, which is crucial for the advancement of numerical models and physical measurement methods.

Hence, this work aims to develop a numerical model of hydraulic jump for a wide range of flow with Froude numbers between 2.00 and 16.00.

Uses of Hydraulic Jump

Hydraulic jumps have numerous practical uses and applications in engineering and water management. Here are some common applications of hydraulic jumps:

- **Energy Dissipation:** Hydraulic jumps are primarily employed to dissipate excess energy in high-velocity flows. They reduce flow velocities, preventing soil erosion and damage to hydraulic structures such as spillways, weirs, and energy dissipaters. By converting kinetic energy into potential energy and turbulence, hydraulic jumps ensure the safe dissipation of energy before water continues downstream. The hydraulic jump for energy dissipation is used in Spillways, Weirs, Dams, etc.
- **Flood Control:** Hydraulic jumps play a critical role in flood control and management. They help regulate the flow of water in rivers, channels, and flood control structures. By dissipating energy and reducing flow velocities, hydraulic jumps prevent excessive erosion, minimize the risk of downstream flooding, and protect infrastructure and communities in flood-prone areas.
- **Sediment Transport:** Hydraulic jumps assist in managing sediment transport in rivers and channels. They influence the movement and deposition of sediment by altering flow velocities and promoting

sediment settling. Hydraulic jumps can help control sedimentation and maintain desired channel morphologies.

- **Water Treatment:** Hydraulic jumps are utilized in water treatment processes. They facilitate the effective mixing of chemicals, such as coagulants or disinfectants, with water. The turbulent mixing in hydraulic jumps enhances the contact between the chemicals and the water, promoting efficient treatment and water disinfection.
- **Fish Passage Design**: Hydraulic jumps are considered in the design of fish passages and fishways, enabling fish to navigate barriers in rivers and dams. The energy dissipation provided by hydraulic jumps ensures suitable flow conditions for fish to pass through without excessive stress or injury.
- **Recreational Activities:** Hydraulic jumps create whitewater features that are popular among enthusiasts of water-based recreational activities such as kayaking, rafting, and surfing. The turbulent and dynamic nature of hydraulic jumps provides opportunities for challenging and thrilling experiences in outdoor settings.

Effect of Hydraulic Jump

Hydraulic jumps have significant effects on the flow and surrounding environment. Here are some key effects of hydraulic jumps:

- **Energy Dissipation:** The primary effect of hydraulic jumps is the dissipation of excess energy in high-velocity flows. As the flow transitions from a supercritical state to a subcritical state, the kinetic energy of the flow is converted into potential energy and turbulence. This dissipation reduces flow velocities, preventing erosion and minimizing the potential for damage to hydraulic structures downstream.
- **Water Surface Elevation Rise:** Hydraulic jumps cause a sudden rise in water surface elevation. This rise in elevation is a result of the conversion of kinetic energy into potential energy during the jump. The higher water surface elevation can have implications for flood control, water level management, and the stability of adjacent areas.
- **Turbulence Generation:** Hydraulic jumps are accompanied by the generation of turbulence. The sudden deceleration and disruption of the flow at the jump result in the formation of turbulent waves and eddies. Turbulence aids in the dissipation of energy and promotes mixing, affecting the transport of sediment, dissolved substances, and heat within the flow.
- **Flow Stabilization**: Hydraulic jumps play a role in stabilizing the flow downstream. The transition from a high-velocity, supercritical flow to a slower, subcritical flow results in a more uniform and stable flow

regime. The turbulent mixing and dissipation in the jump help to achieve a balance between the incoming and downstream flows.

- **Sediment Transport:** Hydraulic jumps can influence sediment transport in rivers and channels. The turbulence generated during the jump affects the movement and deposition of sediment. Sediment particles may settle out or be resuspended within the flow, leading to changes in channel morphology, bed erosion, or deposition.
- **Water Treatment:** Hydraulic jumps are utilized in water treatment processes. The mixing and turbulence generated by hydraulic jumps facilitate the contact and dispersion of chemicals, aiding in processes such as coagulation, flocculation, and disinfection.

  A hydraulic jump frequently forms in natural channels, water treatment facilities, storm water drainage systems, low-head hydraulic structures (such as culverts and weirs), irrigation canals, rivers and canals, industrial applications and manufacturing processes, kitchen sinks as well as in storm streams.

Energy dissipation is yet another application for man-made hydraulic leaps. An illustration of an energy-diminishing use is a hydraulic jump-stilling basin. These basins employ devices like chute blocks, baffle piers, and dentate ends whose efficacy in energy dissipation depends on the Froude number of the entering flow to dissipate up to 60% of the energy of the incoming flow.

Since turbulences like intermittent cavitation, vibration, uplift, and hydrodynamic loading might complicate matters when dealing with heads bigger than 100 meters, hydraulic jump stilling basins are normally not advised for usage in such situations.

These same energy-dissipating principles are also used by other hydraulic structures, such as dams and weirs, to lessen the force of turbulent flows that might scour or damage downstream areas.

While some hydraulic jumps appear like smooth undular waves with almost negligible free-surface turbulence [4], most jumps involve a vigorously tumbling flow region, called the roller.

Their studies focused either on the turbulent water flow properties with relatively low Froude number conditions or on the air-water flow properties in the jump roller.

Experiments

Experimental configuration

Herein, the experimental facilities, a vertical gate provided supercritical inflow. The height of the channel side walls was 2.5 m, such that the maximum inflow velocity was confined to 3.5 m/s. A constant head tank with a

base 2 m x 2 m x 3 m high fed the channel. Discharges up to 250 l/s were run. The tank was divided by a vertical porous wall with Fig. 1. Inlet to (a) channel 3, (b) channels 1 and 4; longitudinal section.

The transition from the tank to the channel was well rounded both along the sidewalls, along the tank bottom to the channel bottom (40 cm above it), and along the vertical, moveable gate. The inlet shape resembled a high-head intake.

Special care was given to the inlet geometry since intake vortices were otherwise generated. The vertical gate could be set in any position between 1 cm and 10 cm above the horizontal channel bottom. The transition between the tank and the channel was improved by a slightly converging cover mounted on the gate.

The length of the cover was 0.4 m; only by such means, a perfect jet (of which the maximum velocity may be as high as 7 m/s) was generated.

The gate slots were closed by small PVC pieces to render the channel inflow geometry continuous. The final result was satisfactory: the inflowing jet to the channel was practically free of turbulence, horizontal, smooth, and free of air bubbles. The first channel portion (1.2 m from the gate) was 500 mm wide. Further, downstream the channel width changed abruptly to 1500 mm.

At the end of this 8 m long reach, a sloping sharp-crested weir allowed adjustment of any desired tail water. The bottom and the right side wall of the 0.70 m high channel were of PVC, the left side of glass. To increase the length of the prismatic channel of width 500 mm to 5 m, two additional sidewalls were inserted.

Further, downstream, it widened to 1500 mm, as previously described. The pump was recalibrated both volumetrically and by a thin crested weir. The discharge thus could be read during the experiments to 0.5 l/s or 1%, whichever was larger. Discharges between 30 l/s and 180 l/s were run. The inflow depth d_1 was read by the gate opening (+ 0.1 mm).

In addition, this depth was also computed from the measured values of discharge Q, and the head in the tank. Deviations between the two values of Q were always smaller than 1 mm. The distance Axj between the cover end and the average position of the jump toe was observed, and the jump inflow depth hx was computed by accounting for wall friction.

All the flows were considered hydraulically smooth. Ax was kept to the minimum, yet without submerging the cover. Typically, Ax was 20 to 30 cm. The sequent flow depth, h_2, was measured both by a point gauge (+ 0.1 mm) and wells which were connected to pressure taps.

Deviations between the two readings were at 1 mm for Fr < 6 and could amount to 5 mm at larger Froude numbers. The end of the surface roller was measured as described by Hager and Bremen (1989): - from the side through the glass wall, using a plumb bob; - from the top, using a point gauge; - with photographs.

The average of at least four measurements was taken and arranged in Appendix 1. The water temperature was always between 16°C and 18°C.

Appendix 1 contains the roller lengths both along the channel axis Lra and along the channel sidewall Lrw. The latter are systematically slightly shorter.

Experimental Flow Conditions

Detailed measurements were conducted for $3.8 < Fr_1 < 8.5$, using an upstream flow depth $d_1 = 0.02$ m. Further experiments were performed with $Fr_1 = 5.1$ for $0.012 \text{ m} < d_1 < 0.047$ m corresponding to $2 \times 10\ 4 < Re < 1.6 \times 10^5$, where $R = \rho \times V_1 \times d_1/\mu$; where ρ is the water density, and μ is the water dynamic viscosity.

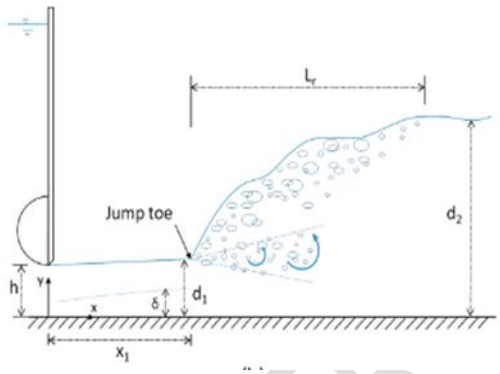

Fig. 1. Experimental facility: flow conditions: Q = 0.0368 m^3/s, $d_1 = 0.0277$ m, $x_1 = 1.083$ m, $Fr_1 = 5.1$, Re =7.4 × 10^4, and flow direction from left to right;

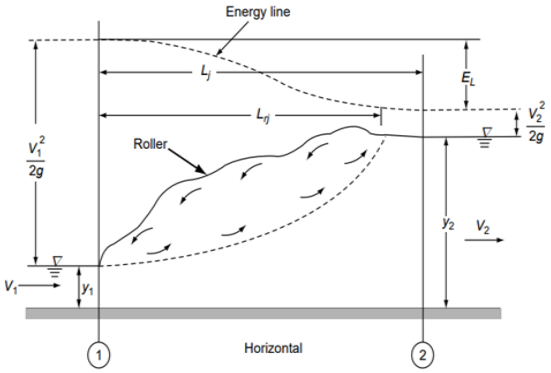

Fig. 2: Definition sketch of a hydraulic jump

The length of roller L_r of a hydraulic jump was observed by various researchers. Non-dimensional roller lengths were presented in which the length scale was either the inflow depth d_1 the sequent depth d_2, or some combination such as $\{h_2 — h_1)$. Since d_2 depends in general on the inflow parameters h_1, Fr_1, Re, and $\omega = d_1/b$ (Hager and Bremen, 1989), the simplest approach for a length measure involves $\lambda_r = L_r/d_1$.

Table 1 summarizes the characteristics of selected experiments of hydraulic jump based on smooth bed condition The Reynolds number is defined as $Re = 4V_1R/\nu$ with V_1 as the velocity and R as hydraulic radius at

the toe of jump, respectively. Characteristics of roller length observation for classical hydraulic jump (ν = 1.1 x 10^{-6} m^2s^{-1}).

Table 1. Characteristics of roller length observation for classical hydraulic jump (ν= 1.1 x 10^{-6} m^2s^{-1})

Author	b (cm)	d_1 (cm)	Fr_1	Re x10^{-5}	Formula
Safranez (1929)	49.9	0.71-5.7	1.72 –19.1	0.58– 2.54	$\lambda_r = 6Fr_1$
Einwachter (1932)	25.0	1.0 – 1.09	2.5– 6.95	0.29– 0.73	-
Pietrkowski (1932)	10.0	0.5 – 1.46	5.5– 19.8	0.83– 1.72	$\lambda_r = 5.9F_{r1}$
Bakhmeteff and Matzke (1936)	15.24	1.0 – 7.75	1.94 – 8.7	0.49– 3.87	Diagram
Schroder (1963)	59.8	3.4 – 10.2	1.83– 9.93	4.44– 10.6	$\lambda_r = 40\text{erf}$
Rajaratnam (1965)	30.8	1.55– 6.13	2.68– 9.78	1.95– 4.19	$\left[\frac{1}{16}(1+8Fr_1^2)^{\frac{1}{2}}-3\right]$
Malik ((1972)	16.7	1.36– 13.18	3 – 6	0.86– 9.88	-
	33.3	1.98– 10.70	3 – 6	1.71– 7.31	-
	50.0	0.66– 18.04	3 – 6	0.35– 17.3	-
Sarma and Newham (1973)	30.5	2.1 – 6.7	1.21– 3.79	1.11– 1.97	-
Hager et al.(1990)	50	5.4 -54.7	2.88-15.96	0.19– 10.2	$\lambda_r = 6.73(F_{r1}-1)$
Murzyn et al (2007)	50	5.4 – 54.7	2.88–5.96	0.19– 10.2	$\lambda_r = 8\left(F_{r1}-\frac{3}{2}\right)$
Kucukali and Chanson (2009)	50	5.4 – 54.7	2.88–5.96	0.19– 10.2	$\lambda_r = -12 + 160tanh(Fr_1/20)$
Hagger et al. (2009)					$\lambda_r = -12 + 100tanh(Fr_1/12.5)$

Leng and Chanson (2015)					λ_r= 8(Fr$_1$ - 1)
Wang and chanson (2015b)					$\lambda_r = 6(F_{r1} - 1)\backslash$
Ozueigbo (2023)			< 2.9 $3.0 - 10.7$ ≥ 10.7		$\lambda_r = 1.3F_{r1}^{1,2}$ $\lambda_r = 4.1F_{r1}^{1,2}$ $\lambda_r = 3.5F_{r1}^{1,2}$

2. Methodology

The author uses the existing rules such as Newton's Law of Motion, the continuity and momentum equations, and the classical hydraulic jump equation to build this model. He uses the equation of motion to calculate the trajectory of an elastic pinball as it bounces off a drop structure with a horizontal step, l, and a height, h, and likes it to the profile of a flow with a hydraulic jump (Fig 3).

3 Formulation of the model

Applying the Law of motion to a bouncing ball between Section 1 and Section 2 gives

$$0 = U_1^2 - 2g(d_2 - d_1)$$

$$U_1 = \sqrt{2g(d_2 - d_1)} \quad (4)$$

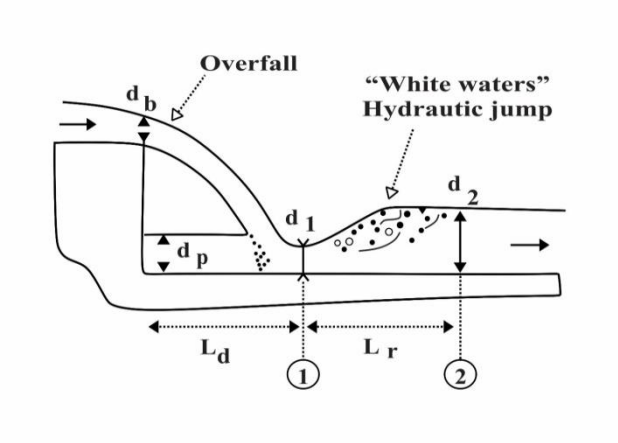

Figure 3: Flow at a drop structure

Where U_1 is the ball rebound velocity at a Section 1,

d_1 is the ball height at Section 1,

d_2 is the ball height at Section 2, and

g is the acceleration due to gravity.

$$0 = \sqrt{2g(d_2 - d_1)} - gt_2$$

$$t_2 = \sqrt{2(d_2 - d_1)/g}$$

Simplifying

$$t_2 = \sqrt{2d_1\,(d_2/d_1 - 1)/g} \tag{5}$$

$$\frac{d_2}{d_1} = \frac{1}{2}\left\{\sqrt{1 + 8Fr_1^2} - 1\right\} \quad (classical\ hydraulic\ jump)$$

$$\frac{d_2}{d_1} - 1 = \left\{0.5\sqrt{1 + 8Fr_1^2} - 1.5\right\} \tag{6}$$

Substituting this well-known classical hydraulic jump formula Eq (6) into Eq (5) and simplifying, yields

$$t_2 = \sqrt{d_1\left(\sqrt{1 + 8Fr_1^2} - 3.0\right)/g} \tag{7}$$

Where t_2 is the time of ball travel from Section 1 to Section 2.

According to Giles et al (1994), for a wide channel with smooth surfaces, the average velocity of flow in a turbulent flow is given as

$$V_{avg} = 2.5v_*\, ln(41.2\, R/\delta) \tag{8}$$

Where V_{avg} is the average velocity between Section 1 and Section 2,

v* the shear velocity is $v_* = \sqrt{gSR}$ (9)

R is the hydraulic radius, which for a wide channel is d_1. and

δ the thickness of the boundary layer is $\delta = 11.6\,\nu/v_*$ (10)

where υ is the kinetic viscosity of water and g is the acceleration due to gravity,

S the water surface relative to the channel slope is $S = (d_2 - d_1)/L_r$ or $d_1(d_2/d_1 - 1)/L_r$ (11)

Where d_2 is the flow depth at Section 2 and d_1 is the flow at Section 1 and

Lr is the roller length of the hydraulic jump,

Substituting Equations (9), (10), and (11) into Eq (8) and simplifying, yields

$$V_{avg} = 2.5\sqrt{gSd_1}\; ln\left(41.2\, d_1\sqrt{gSd_1}/11.6\upsilon\right)$$

$$V_{avg} = 2.5\sqrt{g d_1 \frac{d_1(d_2/d_1 - 1)}{L_r}}\; ln\left(41.2 d_1 \frac{\sqrt{g d_1\, d_1(d_2/d_1 - 1)/L_r}}{11.6\upsilon}\right)$$

$$V_{avg} = 2.5 d_1\sqrt{\frac{g(d_2/d_1 - 1)}{L_r}}\; ln\left(41.2 d_1^2 \frac{\sqrt{g\,(d_2/d_1 - 1)/L_r}}{11.6\upsilon}\right) \quad (12)$$

$$L_r = V_{avg}\, t_2 \quad (13)$$

Substituting Equations (7) and (12) into Eq (13) and dividing by d_1, and simplifying yields Eq (14).

$$L_r = 2.5 d_1\sqrt{\frac{g(d_2/d_1 - 1)}{L_r}}\; ln\left(41.2 d_1^2 \frac{\sqrt{g\,(d_2/d_1 - 1)/L_r}}{11.6\upsilon}\right)\sqrt{2d_1\,(d_2/d_1 - 1)/g}$$

$$\frac{Lr}{d_1} = 2.5\sqrt{\frac{g(d_2/d_1 - 1)}{L_r}}\; ln\left(41.2 d_1^2 \frac{\sqrt{g\,(d_2/d_1 - 1)/L_r}}{11.6\upsilon}\right)\sqrt{2d_1\,(d_2/d_1 - 1)/g}$$

$$\frac{Lr}{d_1} = 2.5\sqrt{\frac{g(d_2/d_1 - 1)}{L_r}}\; ln\left(41.2 d_1^2 \frac{\sqrt{g\,(d_2/d_1 - 1)/L_r}}{11.6\upsilon}\right)\sqrt{2d_1\,(d_2/d_1 - 1)/g}$$

$$\frac{Lr}{d_1}\sqrt{\frac{L_r}{d_1}}\sqrt{ln\frac{L_r}{d_1}}\sqrt{ln\frac{1}{d_1^3}}$$

$$= 2.5\sqrt{g\left(0.5\sqrt{1 + 8Fr_1^2} - 1.5\right)}\; ln\left(41.2\frac{\sqrt{g\left(0.5\sqrt{1 + 8Fr_1^2} - 1.5\right)}}{11.6\upsilon}\right)\sqrt{\left(\sqrt{1 + 8Fr_1^2} - 3.0\right)/g}$$

$$\frac{Lr}{d_1}\sqrt{\frac{L_r}{d_1}}\sqrt{ln\frac{L_r}{d_1}}\sqrt{ln}\left(\frac{Lr^0}{d_1}\right)^3$$

$$= 2.5\sqrt{g\left(0.5\sqrt{1 + 8Fr_1^2} - 1.5\right)}\; ln\left(41.2\frac{\sqrt{g\left(0.5\sqrt{1 + 8Fr_1^2} - 1.5\right)}}{11.6\upsilon}\right)\sqrt{\frac{\left(\sqrt{1 + 8Fr_1^2} - 3.0\right)}{g}}$$

$$\sqrt{\left(\frac{Lr}{d_1}\right)^3}\sqrt{ln\left(\frac{L_r}{d_1}\right)}\sqrt{ln\left(\frac{1}{d_1}\right)^3}$$

$$= 2.5\sqrt{g\left(0.5\sqrt{1\ +\ 8Fr_1^2}\ -\ 1.5\right)}\ ln\left(41.2\frac{\sqrt{g\left(0.5\sqrt{1\ +\ 8Fr_1^2}\ -\ 1.5\right)}}{11.6\upsilon}\right)\sqrt{\frac{\left(\sqrt{1\ +\ 8Fr_1^2}\ -\ 3.0\right)}{g}}$$

$$\sqrt{\left(\frac{Lr}{d_1}\right)^3}\sqrt{ln\left(\frac{L_r}{d_1}\right)}\sqrt{ln\left(\frac{1}{d_1}\right)^3}$$

$$= 2.5\sqrt{g\left(0.5\sqrt{1\ +\ 8Fr_1^2}\ -\ 1.5\right)}\sqrt{\frac{\left(\sqrt{1\ +\ 8Fr_1^2}\ -\ 3.0\right)}{g}}ln\left(41.2\frac{\sqrt{g\left(0.5\sqrt{1\ +\ 8Fr_1^2}\ -\ 1.5\right)}}{11.6\upsilon}\right)$$

$$\sqrt{\left(\frac{Lr}{d_1}\right)^3}\sqrt{ln\left(\frac{L_r}{d_1}\right)}\sqrt{ln\left(\frac{Lr^0}{d_1}\right)^3}$$

$$= 2.5\sqrt{\left(0.5\sqrt{1\ +\ 8Fr_1^2}\ -\ 1.5\right)}\left(\sqrt{1\ +\ 8Fr_1^2}\right.$$

$$\left.-\ 3.0\right)ln\left(41.2\frac{\sqrt{g\left(0.5\sqrt{1\ +\ 8Fr_1^2}\ -\ 1.5\right)}}{11.6\upsilon}\right)$$

$$\sqrt{\left(\frac{Lr}{d_1}\right)^3}\sqrt{ln\left(\frac{L_r}{d_1}\right)}\sqrt{ln\left(\frac{Lr^0}{d_1}\right)^3}$$

$$= 2.5\sqrt{\left(0.5\sqrt{1\ +\ 8Fr_1^2}\ -\ 1.5\right)\left(\sqrt{1\ +\ 8Fr_1^2}\ -\ 3.0\right)}ln\left(41.2\frac{\sqrt{g\left(0.5\sqrt{1\ +\ 8Fr_1^2}\ -\ 1.5\right)}}{11.6\upsilon}\right)$$

$$\sqrt{\left(\frac{Lr}{d_1}\right)^3}\sqrt{ln\left(\frac{L_r}{d_1}\right)}\sqrt{ln\left(\frac{Lr^0}{d_1}\right)^3}$$

$$= 2.5\sqrt{\left(0.5(1\ +\ 8Fr_1^2) + 1.5\sqrt{1\ +\ 8Fr_1^2} +\ 3.0\sqrt{1\ +\ 8Fr_1^2}\ -\ 4.5\right)}ln\left(41.2\frac{\sqrt{g\left(0.5\sqrt{1\ +\ 8Fr_1^2}\ -\ 1.5\right)}}{11.6\upsilon}\right)$$

$$\sqrt{\left(\frac{Lr}{d_1}\right)^3}\sqrt{ln\left(\frac{L_r}{d_1}\right)}\sqrt{ln\left(\frac{Lr^0}{d_1}\right)^3}$$

$$= 2.5\sqrt{\left(0.5(1 + 8Fr_1^2) + 4.5\sqrt{1 + 8Fr_1^2} - 4.5\right)}ln\left(41.2\frac{\sqrt{g\left(0.5\sqrt{1 + 8Fr_1^2} - 1.5\right)}}{11.6\upsilon}\right) \quad (14)$$

Eq (14) is valid for $3.96 \leq Fr_1 \leq 15.96$

$$\sqrt{\left(\frac{Lr}{d_1}\right)^3}\sqrt{ln\left(\frac{L_r}{d_1}\right)}\sqrt{ln\left(\frac{Lr^0}{d_1}\right)^3}$$

$$= 1.0\sqrt{\left(0.5(1 + 8Fr_1^2) + 4.5\sqrt{1 + 8Fr_1^2} - 4.5\right)}ln\left(41.2\frac{\sqrt{g\left(0.5\sqrt{1 + 8Fr_1^2} - 1.5\right)}}{11.6\upsilon}\right) \quad (15)$$

Eq (15) is valid for $2.38 \leq Fr_1 \leq 3.96$

4. Verification of the Developed Model

The author verifies the developed model with the experimental data and the results are presented below

5. RELATIONSHIP BETWEEN MEASURED AND ESTIMATED DIMENSIONLESS HYDRAULIC JUMP AND FROUDE NUMBER AT THE JUMP TOE

Figure 4a through Figure 4g show the comparison of the measured and estimated dimensionless hydraulic jump with the Froude numbers at the toe of the hydraulic jump. The figures show that the measured and the estimated dimensionless hydraulic jump increase rapidly with increasing Froude Numbers, which is in line with reports recorded in the literature.

The figures also shows that all the measured dimensionless hydraulic jump data compare well with Eq (14) and Eq (15) - the developed model dimensionless hydraulic jump model data with the Pearson correlation coefficients of between 0.992 and 0.997.

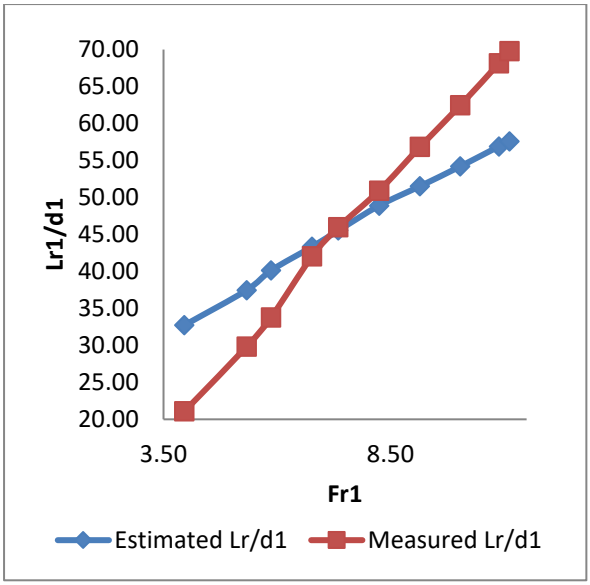

Figure 4a: Measured dimensionless hydraulic roller length as a function of the Froude number between 3.96 and 11.12 & d_1 between 27.5 and 34.1. Comparison with Eq (14) (the Developed Model).

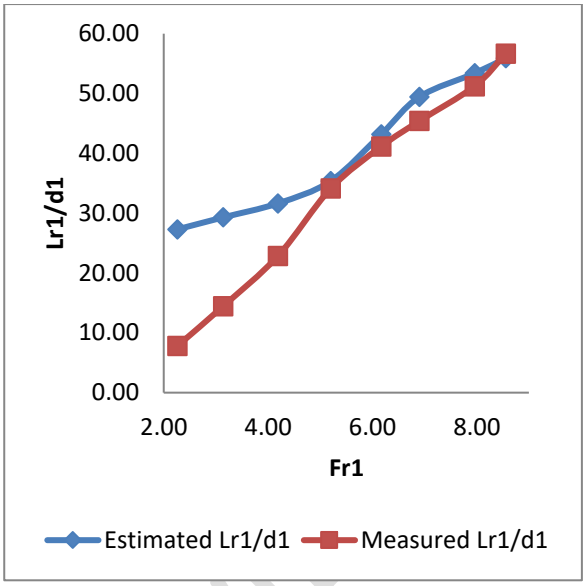

Figure 4b: Measured dimensionless hydraulic roller length as a function of the Froude number between 2.26 and 8.56 & d_1 between 48.8 and 54.7. Comparison with Eq (14) (the Developed Model).

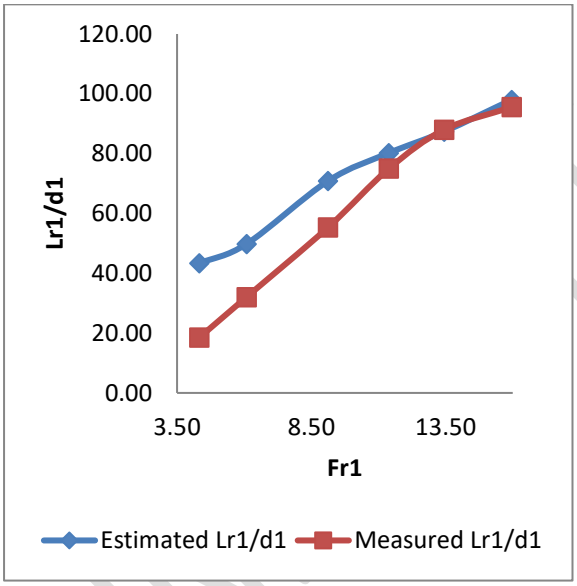

Figure 4c: Measured dimensionless hydraulic roller length, Lr/d_1 as a function of the Froude number, Fr_1 between 4.33 and 15.36 & d_1 between 5.4 and 4.5. Comparison with Eq (14) (the Developed Model).

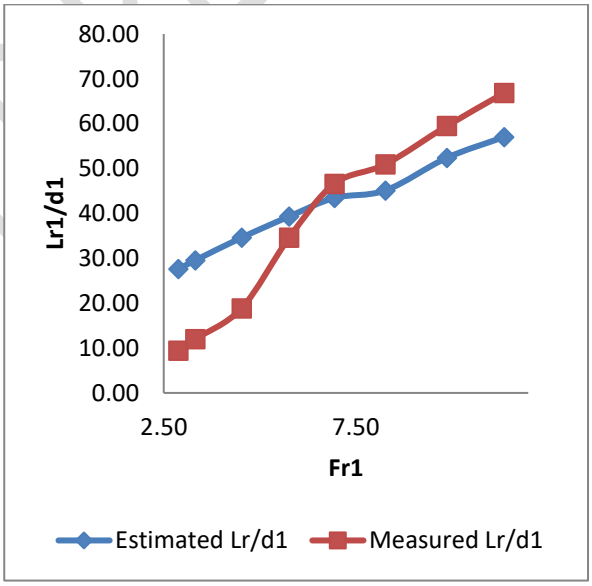

Figure 4d: Measured dimensionless hydraulic roller length, Lr/d_1 as a function of the Froude number, Fr_1 between 2.88 and 11.37 & d_1 between 10.6 and 9.8. Comparison with Eq (14) (the Developed Model).

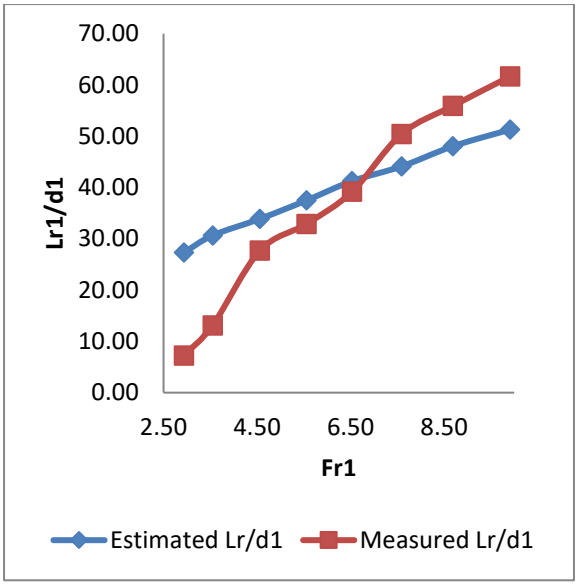

Figure 4e: Measured dimensionless hydraulic roller length, Lr/d_1 as a function of the Froude number, Fr_1 between 2.94 and 9.91 & d_1 between 12.4 and 11.0. Comparison with Eq (14) (the Developed Model).

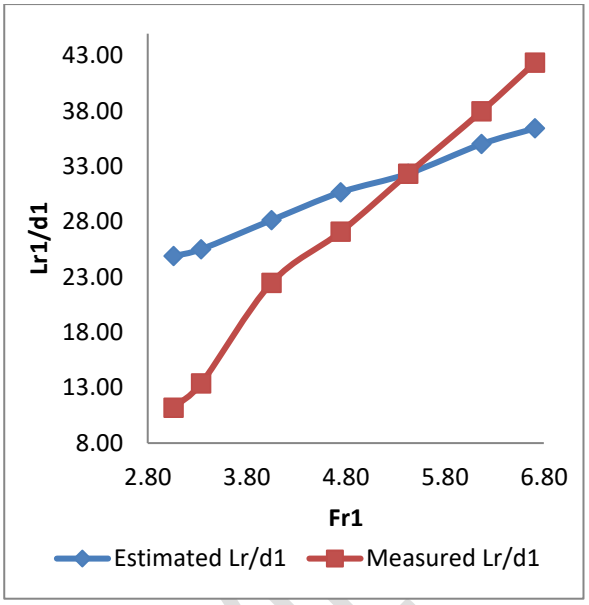

Figure 4f: Measured dimensionless hydraulic roller length, Lr/d_1 as a function of the Froude number, Fr_1 between 3.06 and 6.71 & d_1 between 24.1 and 23.8. Comparison Eq (15)(Developed Model).

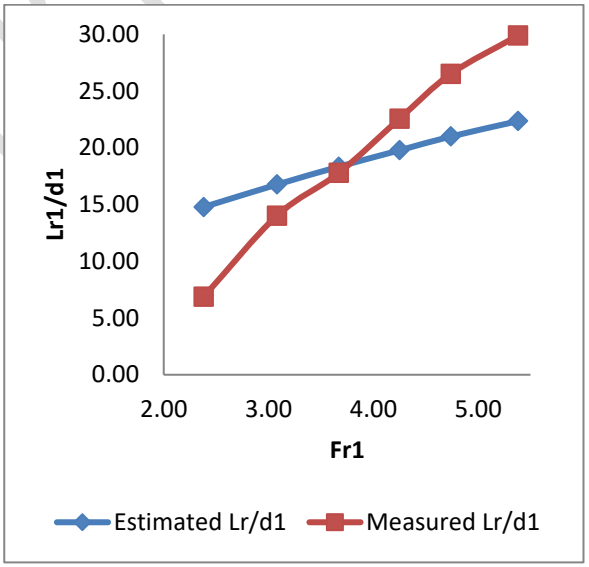

Figure 4g: Measured dimensionless hydraulic roller length, Lr/d_1 as a function of the Froude number, Fr_1 between 2.38 and 5.38 & d_1 between 37.9 and 35.8. Comparison Eq (15) (the Developed Model).

6. RELATIONSHIP BETWEEN THE MEASURED DIMENSIONLESS HYDRAULIC JUMP LENGTH AND THE ESTIMATED DIMENSIONLESS HYDRAULIC JUMP LENGTH.

Figure 5a through Figure 5g show the comparison of the measured and estimated dimensionless hydraulic jump with the Froude numbers of the hydraulic jump. The figures show that all the measured dimensionless hydraulic

jump data compare well with Eq (14) and Eq (15) - the developed model dimensionless hydraulic jump model data with the Pearson correlation coefficients of between 0.992 and 0.997.

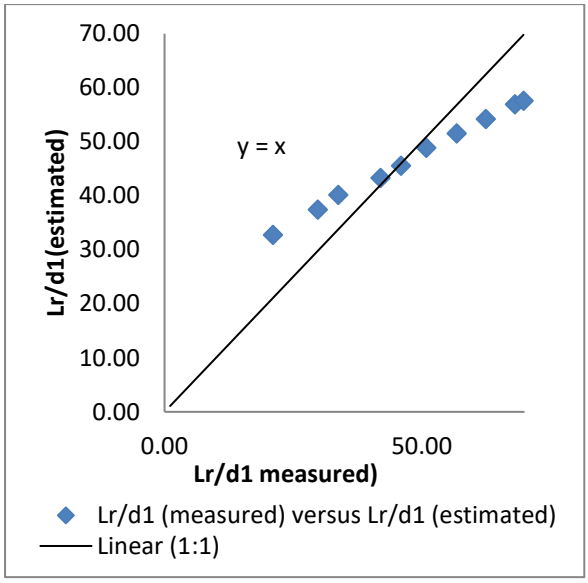

Figure 5a: Lr_1/d_1(measured) as a function of Lr_1/d_1(estimated) for Lr_1/d_1(measured) between 21.1 and 69.8 and 57.8 and Lr_1/d_1 (estimated) between 32.7 and 57.8.

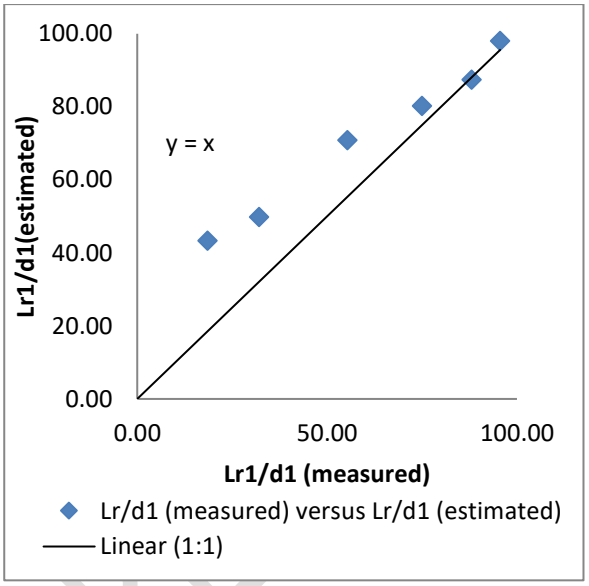

Figure 5c: Lr_1/d_1 (measured) as a function of Lr_1/d_1 (estimated) for Lr_1/d_1 (measured) between 18.5 and 95.6 & Lr_1/d_1 (estimated) between 43.3 and 98.0.

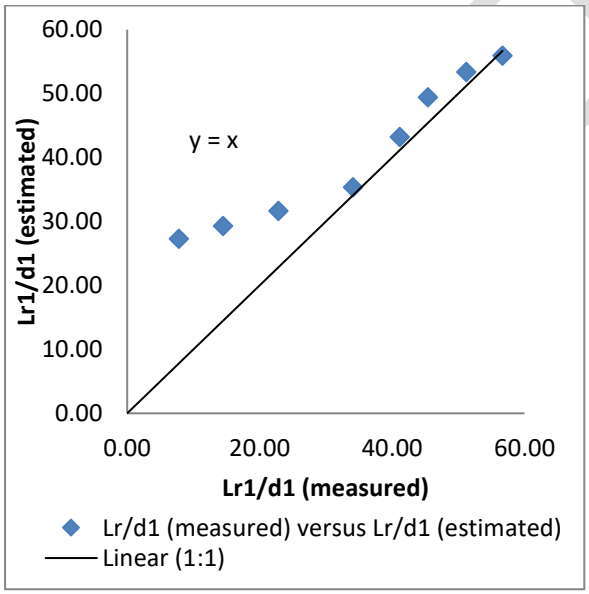

Figure 5b: Lr_1/d_1 (measured) as a function of Lr_1/d_1 (estimated) for Lr_1/d_1 (measured) between 7.8 and 56.9 & Lr_1d_1 (estimated) between 27.3 and 57.9.

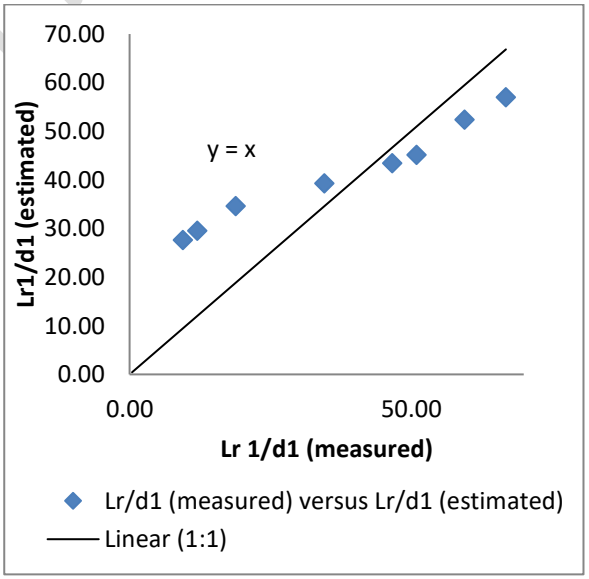

Figure 5d: Lr_1 /d_1 (measured) as a function of Lr_1/d_1 (estimated) for Lr_1/d_1 (measured) between 9.4 and 66.8 & Lr_1/d_1 (estimated) between 27.6 and 57.0.

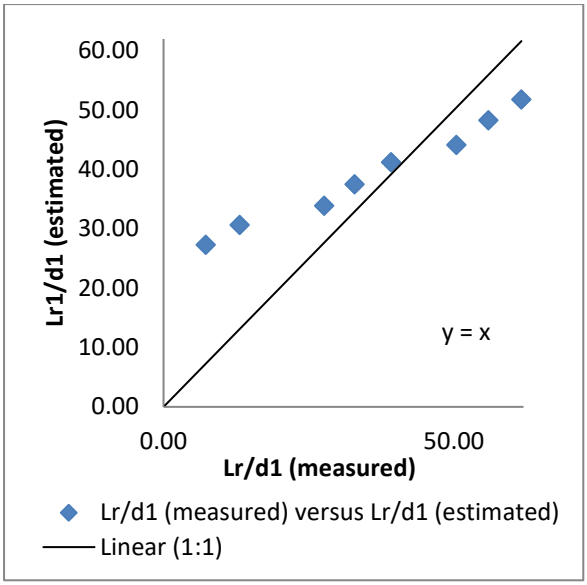

Figure 5e: Lr_1 (measured)/d_1 as a function of Lr_1 (estimated)/d_1 for Lr_1 (measured)/d_1 between 7.8 and 61.6 & Lr_1 (estimated)/d_1 between 27.8 and 51.3.

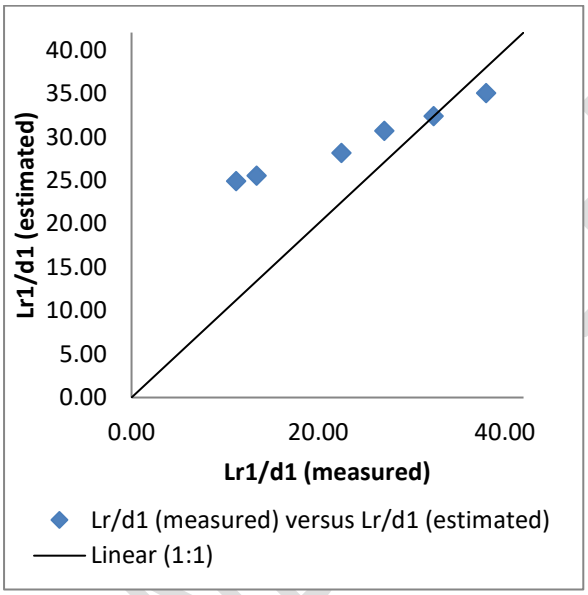

Figure 5f: Lr_1/d_1 (measured) as a function of Lr_1 /d_1 (estimated) for Lr_1d_1 (measured) between 11.2 and 42.4 & Lr_1 /d_1(estimated) between 27.8 and 41.6.

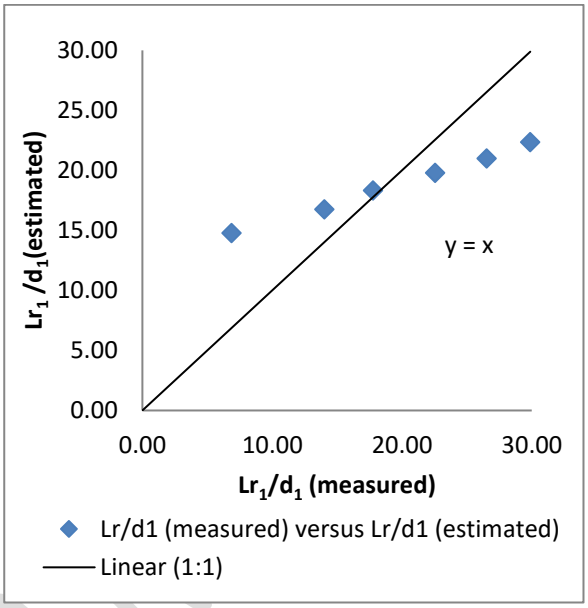

Figure 5g: Lr_1/d_1 (measured) as a function of Lr_1/d_1 (estimated) for Lr_1/d_1 (measured) between 6.9 and 29.9 & Lr_1/d_1 (estimated) between 26.5 and 39.5.

7. RELATIONSHIP BETWEEN THE MEASURED DIMENSIONLESS HYDRAULIC JUMP LENGTH AND THE ESTIMATED HYDRAULIC JUMP.

Figure 6a through Figure 6g show the comparison of the measured and estimated hydraulic jump. The figures show that all the measured hydraulic jump data compare well with Eq (14) and Eq (15) - the developed model dimensionless hydraulic jump model data with the Pearson correlation coefficients of between 0.993 and 0.995.

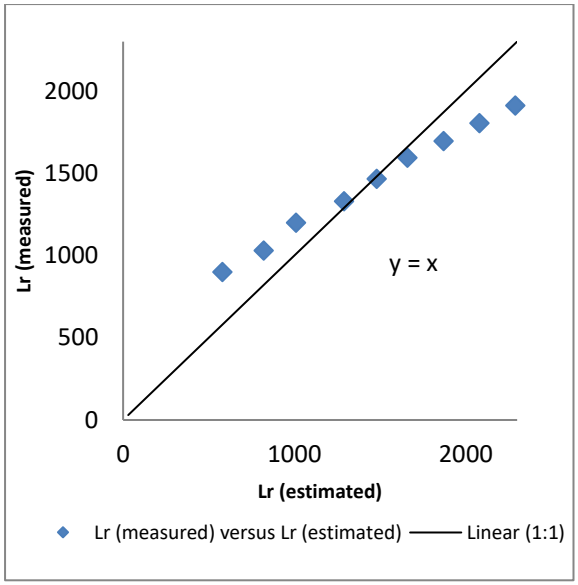

Figure 6a: Lr_1 (estimated) as a function of Lr_1 (measured) for Fr_1 between 3.96 and 11.12 & d_1 between 27.5 and 34.1

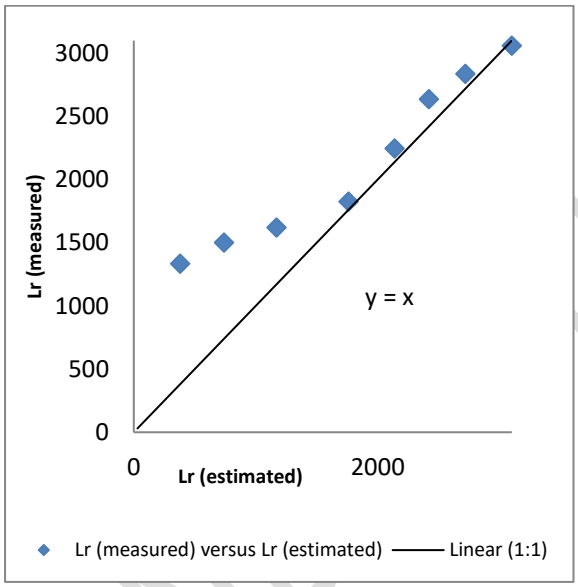

Figure 6b: Lr_1 (estimated) as a function of Lr_1 (measured) for Fr_1 between 2.26 and 8.56 & d_1 between 48.8 and 54.7

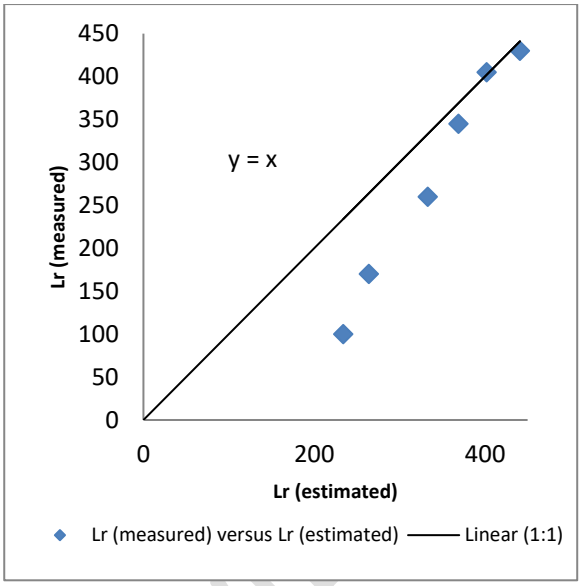

Figure 6c: Lr_1 (estimated) as a function of Lr_1 (measured) for Fr_1 between 4.33 and 15.36 & d_1 between 5.4 and 4.5.

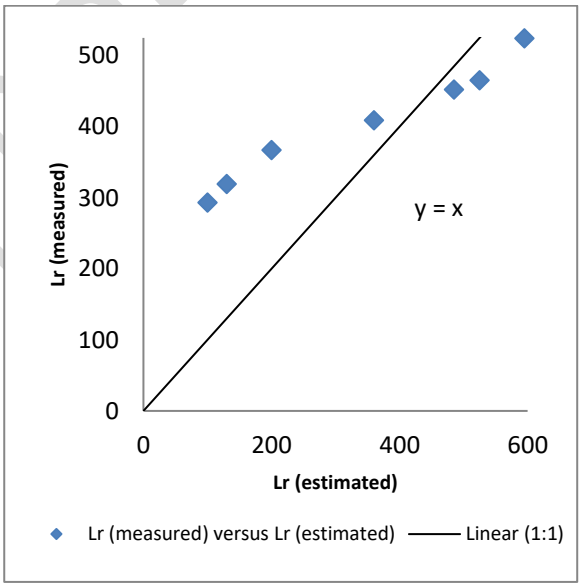

Figure 6d: Lr_1 (estimated) as a function of Lr_1 (measured) for Fr_1 between 2.88 and 11.37 & d_1 between 10.6 and 9.8

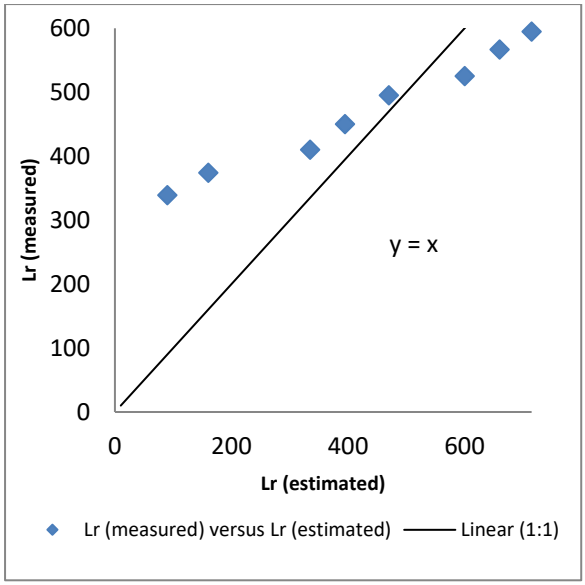

Figure 6e: Lr_1 (estimated) as a function of Lr_1 (measured) for Fr_1 between 2.94 and 9.91 & d_1 between 12.4 and 11.0

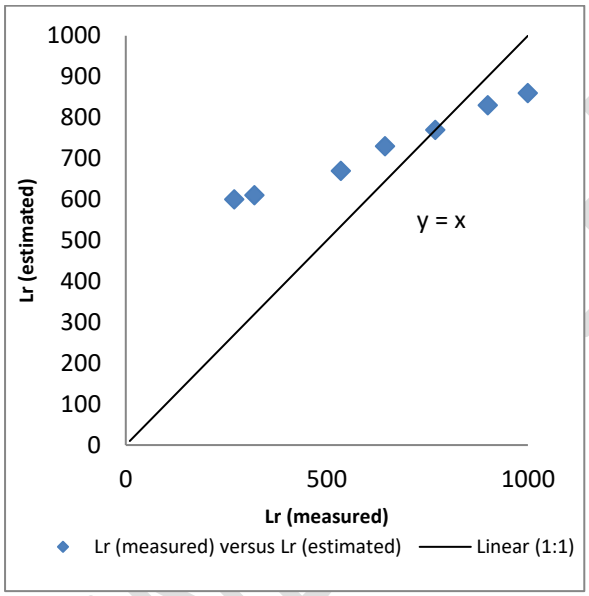

Figure 6f: Lr_1 (estimated) as a function of Lr_1 (measured) for Fr_1 between 3.06 and 6.71 & d_1 between 24.1 and 23.8

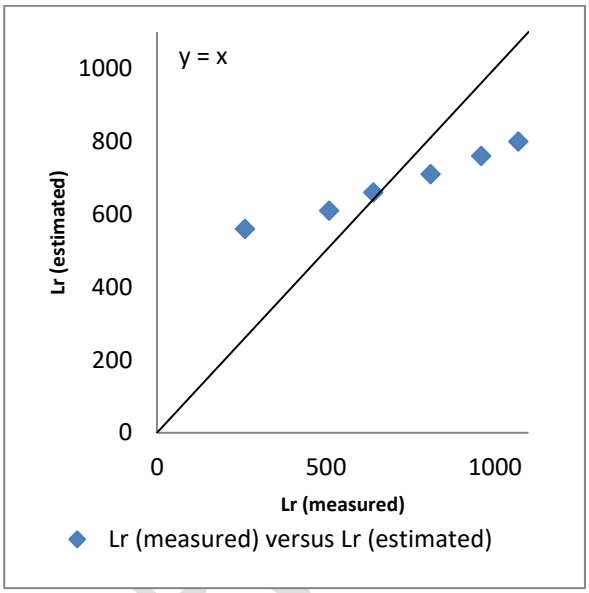

Figure 6g: Lr_1 (estimated) as a function of Lr_1 (measured) Fr_1 between 2.38 and 5.38 & d_1 between 37.9 and 35.8

8 Results and Discussions

Results showed that two new models were developed to analytically calculate the length of a hydraulic jump in a horizontal open channel flow using a bouncing ball. The models were based on the laws of motion and the principles of impulse and momentum, to predict the length of a hydraulic jump in a horizontal open channel flow with the Froude number between 2.25 and 15.96. The models were then verified with the experimental data obtained in a large-size facilities. The measured and the estimated dimensionless hydraulic jump were virtually identical with each other and increase rapidly with the increasing Froude Numbers, which is in line with reports recorded in the literature. The values of the hydraulic jumps were also reasonable estimated from Eq (14) and Eq

(15) - the developed model dimensionless hydraulic jump model data with the Pearson correlation coefficients of between 0.992 and 0.997.

LISTS OF SYMBOLS

e – coefficient of restitution (COR) assumed constant and less than 1 because of the elastic bounce of ball;
d_c – critical height of ball (m);
d_o - uniform ball depth at the weir (m);
Fr - Froude Number;
h - step height (m), which is also equals to the head loss at any intermediary step ;
V_b - incident ball velocity (m/s^2);
V_c - critical ball velocity (m/s^2)
x, y – x, and y axes coordinates of ball for all bounces with origin fixed at the weir(m);
H_1 – residual head at the bottom of the spillway (m);
ΔH – difference between the maximum head and the residual head (m);
H - total head (m);
H_{max} - maximum head available (m):
$H_{max} = H_{dam} + 3/2 * d_c$;
Hres - residual head at the bottom of the spillway (m);
h - height of steps (m);
l - horizontal length of steps (m);
Q - discharge (m^3/s);
q - discharge per unit width (m^2/s);
Reynolds number defined as : $Re = \rho_w * U_w * D_H / \mu_w$
Uw - flow velocity (m/s): $U_w = q_w/d$;
W - channel width (m);
ΔH - head loss (m);
μ - dynamic viscosity ($N.s/m^2$);
ρ - density (kg/m^3);

Subscript
a – conditions at ball bounce;
b – conditions at step brink;
c – conditions at critical height;
d – conditions at maximum ball height;
N– number of step;

REFERENCES

[1] RV Giles, JB Evett, Ph.D and C Liu. Schaum's Outline of Fluid Mechanics and Hydraulics, Series, McGrawHill Press, New York, 3rd Edition, 1994, p. 200-202
[2] Boes, R. M. (2000). Scale effects in modeling two phase stepped spillway flow. In *Proc. Intl. Workshop on Hydraulics of Stepped Spillways*, 53 - 60. H. E. Minor and W. H. Hager, eds. Steenwijk, the Netherlands: A. A. Balkema.
[3] Boes, R. M., and Hager, W. H. (1998). Fiber optical experimentation in two phase cascade flow. In *Proc. Intl. RCC Dams Seminar*. K. Hanson, ed. Denver, Colo.: Schnabel Engineering.
[4] Chanson, H and Toobes L, ''Flow Patterns in Nappe Flow Regime Down Low Gradient Stepped Chutes''. Journal of Hydraulic Research No 46, No 1 (2008), pp 4 – 44 @ International Association of Hydraulic Engineering and Research.
[5] Felder, S., and Chanson, H. (2008). Turbulence and turbulent length and time scales in skimming flows on a stepped spillway: Dynamic similarity, physical modeling, and scale effects. Queensland, Australia: University of Queensland, Division of Civil Engineering.
[6] CAROSI, G. and CHANSON, H. (2006). "Air-Water Time and Length Scales in Skimming Flows on a Stepped Spillway. Application to the Spray Characterisation." Report No. CH59/06, Div. of Civil Engineering, The University of Queensland, Brisbane, Australia, July, 142 pages (ISBN 1864998601).
[7] Chanson, H. Hydraulics of Nappe Flow Regime Above Stepped Chutes And Spillways

[8] Chanson, H. (2002). *The Hydraulics of Stepped Chutesand Spillways.* Steenwijk, The Netherlands: A. A. Balkema.
[9] Chanson, H., and Toombes, L. (2002). Energy dissipation and air entrainment in a stepped storm waterway: An experimental study. *J. Irrig. and Drainage Eng. ASCE* 128(5): 305- 315.
[10] Chanson, H.(2002) *The Hydraulics of Stepped Chutes and Spillways.* Lisse, the Netherlands: Balkema.
[11] Chanson, H (2002), Hydraulics of Stepped Spillways: Current Status, *Journal of Hydraulic Engineering,* 126(9), 2000, pp. 636-637.
[12] Chanson, H. (2000). Characteristics of skimming flow over stepped spillways: Discussion. *J. Hydraul. Eng. ASCE* 125(4): 862- 865.
[13] Chanson, H (1997). ''Model Study of a Roller Compacted Concrete Stepped Spillway.'' Journal of Hydraulic Engineering, ASCE, Vol 123, No 10, pp, 931- 933 (ISSN 0733 – 9429).
[14] Chanson, H. (1996). ''Prediction of the Transition Nappe/Skimming Flow On a Stepped Channel' Journal of Hydraulic Research, Vol. 34, 1996 No 3.
[15] Chanson, H (1994), Comparison of energy dissipation between nappe and skimming flow regimes on stepped chutes, *Journal of hydraulic research,*32 (2), 1994, pp. 213–218.
[16] Chanson, H. (1994a). Hydraulics of skimming flows over stepped channels and spillways. *IAHR J. Hydraul. Res.* 32(3): 445- 460.
[17] Chanson, H. (1994b). *Hydraulic Design of Stepped Cascades, Channels, Weirs, and Spillways*. Oxford, U.K.: Pergamon.
[18] Chanson, H (1994), ''Hydraulics of Nappe Flow Regime above Stepped Chutes and Spillways'' Aust, Civil Engg Tranports, I, E, Aust, CE 36 (1), 69 -76
[19] CHANSON, H. (1993). "Stepped Spillway Flows and Air Entrainment." *Can. Jl of Civil Eng.*, Vol. 20, No. 3, June, pp. 422-435 (ISSN 0315-1468). JOURNAL DE RECHERCHES HYDRAUUQUES, VOL. 34, 1996, *'Vol.* 3 Prediction of the transition nappe/skimming flow on a stepped channel
[20] Chanson, H (1988), ''A Study of Air Entrainment and Aeration Devices on a Spillway Model''. Ph.D Thesis, Ref 88 – 8, ''Department of Civil Engineering University of Canterbury, New Zealand. Hydraulic of Nappe Flow Regime Above Stepped Chute and Spillways
[21] Chow, V. T. (1959). *Open Channel Hydraulics.* Boston, Mass.: McGrawHill.
[22] Christodoulou, G. C. (1993). Energy dissipation on stepped spillways. *J. Hydraul. Eng. ASCE* 119(5): 644- 655.
[23] Cross R 2019 Rolling over an obstacle Eur. J. Phys.
[24] Cross Rodney and Crawford Lindsey (2019), Collision of a ball with the edge of a step,European Journal of Physics
[25] Cross R 2019 Rolling over an obstacle Eur. J. Phys. 40 Cross R 2010 The polar moment of inertia of striking implements Sports Technology 3 215–9 [9] Cross R and Nathan A 2007 Experimental study of the gear effect in ball collisions Am. Jnl Phys. 75
[26] FELDER, S. and CHANSON, H. (2012). "Air-Water Flow Measurements in Instationary Free Surface Flows: a Triple Decomposition Technique." Hydraulic Model Report No. CH85/12, School of Civil Engineering, The University of Queensland, Brisbane, Australia
[27] FELDER, S. and CHANSON, H. (2011a). "Air-Water Flow Properties in Step Cavity down a Stepped Chute." International Journal of Multiphase Flow, Vol.
[29] FELDER, S. and CHANSON, H. (2011b). "Energy Dissipation down a Stepped Spillway with Non Uniform Step Heights." Journal of Hydraulic Engineering, ASCE, Vol. 137, No. 11, pp. 1543- 1548 (DOI 10.1061/(ASCE)HY.1943-7900.0000455).
[30] FELDER, S. and CHANSON, H. (2009b). "Turbulence, Dynamic Similarity and Scale Effects in High-Velocity Free-Surface Flows above a Stepped Chute." Experiments in Fluids, Vol. 47, No. 1, pp. 1-18. *2006 World Environ. and Water Resources Congress, ASCE Conf*., CD-ROM. Reston, Va.: ASCE.
[31] Márton Gruiz , Tamás Meszéna2 and Tamás Tél (2017), Chaotic or just complicated? Ball bouncing own the stairs, IOP Publishing, European Journal of Physics, Eur. J. Phys. 38 (2017) 055003 (15pp)
[32] Peyras, L., P. Royet, and Degoutte, G. (1992). Flow and energy dissipation over stepped gabion weirs. *J. Hydraul. Eng. ASCE*118(5): 707-717.
[33] Rice, C. E., and Kadavy, K. C. (1996). Model study of a roller compacted concrete stepped spillway. *J. Hydraul. Eng. ASCE*122(6): 92- 297.

Appendix1:

1

t-Test: Paired Two Sample for Means

	Variable 1	*Variable 2*
Mean	46.82564	48.08417
Variance	71.44726	274.866
Observations	10	10
Pearson Correlation	0.999012	
Hypothesized Mean Difference	0	
df	9	
t Stat	-0.48871	
P(T<=t) one-tail	0.318366	
t Critical one-tail	1.833113	
P(T<=t) two-tail	0.636732	
t Critical two-tail	2.262157	

2

t-Test: Paired Two Sample for Means

	Variable 1	*Variable 2*
Mean	40.69291	34.20677
Variance	127.9358	312.1576
Observations	8	8
Pearson Correlation	0.969272	
Hypothesized Mean Difference	6	
df	7	
t Stat	0.189419	
P(T<=t) one-tail	0.42757	
t Critical one-tail	1.894579	
P(T<=t) two-tail	0.85514	
t Critical two-tail	2.364624	

3

t-Test: Paired Two Sample for Means

	Variable 1	*Variable 2*
Mean	40.69291	34.20677
Variance	127.9358	312.1576
Observations	8	8
Pearson Correlation	0.969272	
Hypothesized Mean Difference	6	
df	7	
t Stat	0.189419	
P(T<=t) one-tail	0.42757	

t Critical one-tail	1.894579
P(T<=t) two-tail	0.85514
t Critical two-tail	2.364624

4

t-Test: Paired Two Sample for Means

	Variable 1	*Variable 2*
Mean	71.60074	60.75203
Variance	458.9793	958.9288
Observations	6	6
Pearson Correlation	0.993412	
Hypothesized Mean Difference	6	
df	5	
t Stat	1.188838	
P(T<=t) one-tail	0.143941	
t Critical one-tail	2.015048	
P(T<=t) two-tail	0.287882	
t Critical two-tail	2.570582	

t-Test: Paired Two Sample for Means

	Variable 1	*Variable 2*
Mean	41.14701	37.36207
Variance	109.0941	485.8482
Observations	8	8
Pearson Correlation	0.98682	
Hypothesized Mean Difference	6	
df	7	
t Stat	-0.52844	
P(T<=t) one-tail	0.306764	
t Critical one-tail	1.894579	
P(T<=t) two-tail	0.613529	
t Critical two-tail	2.364624	

5

t-Test: Paired Two Sample for Means

	Variable 1	*Variable 2*
Mean	39.26129	36.01655
Variance	71.1111	385.861
Observations	8	8
Pearson Correlation	0.991562	
Hypothesized Mean Difference	0	
df	7	
t Stat	0.809691	
P(T<=t) one-tail	0.222383	

t Critical one-tail	1.894579
P(T<=t) two-tail	0.444766
t Critical two-tail	2.364624

6

t-Test: Paired Two Sample for Means

	Variable 1	*Variable 2*
Mean	34.712	26.69611
Variance	27.11856	140.0029
Observations	7	7
Pearson Correlation	0.998362	
Hypothesized Mean Difference	8	
df	6	
t Stat	0.006331	
P(T<=t) one-tail	0.497577	
t Critical one-tail	1.94318	
P(T<=t) two-tail	0.995154	
t Critical two-tail	2.446912	

7

t-Test: Paired Two Sample for Means

	Variable 1	*Variable 2*
Mean	33.44733	19.6032
Variance	23.37636	71.87283
Observations	6	6
Pearson Correlation	0.998376	
Hypothesized Mean Difference	14	
df	5	
t Stat	-0.10429	
P(T<=t) one-tail	0.460497	
t Critical one-tail	2.015048	
P(T<=t) two-tail	0.920995	
t Critical two-tail	2.570582	

8

9

10

11

12